STRAIN GAGE AS A DISPLACEMENT TRANSDUCER

Cajuhi, Aguinaldo Jose, ajcajuhi@bol.com.br
Pepe, Iuri Muniz, mpepe@ufba.br
Laboratório de Propriedades Óticas, Instituto de Fisica, Universidade Federal da Bahia – UFBA, PPGM, Escola Politécnica,
Universidade Federal da Bahia – UFBA

Abstract. The firsts concerns on choosing a transducer are: cost, accuracy, response to excitation, repeatability, measurement reproducibility, building and installation easiness, mechanical housing complexity and maintenance. When one requires high accuracy and precise excitation response the cost of transducer grows, from hundreds to thousands dollars. For displacement transduction many technologies are available, as well as the way of installing that kind of transducer on a given mechanical system. On this work it is presented the methodology to develop a displacement transducer based on strain gage. As strain gage is sensitive to very small deformations, we proposed using mechanical devices, based on elastic components, to amplify the small variation and built a final transducer capable of measuring up to 250 mm displacement. It is also discussed the method to calibrate the proposed device.

Keywords: strain gage; displacement transducer; deformation; calibration

1. INTRODUCTION

Load cells (LC) can be used as force, displacement, torque and pressure transducers, being able to be applied in many situations due to its great diversity of models and forms, combined with its small dimensions. The LC principle of functioning is normally based on the linear resistance variations suffered by the strain gage, also called strain gages, when it is submitted to an elastic mechanical deformation.

The majority of the load cells are manufactured with four electric strain gages connected as a balanced Wheatstone bridge. This kind of configuration enlarges the electric signals on the measuring, allowing high sensibility on the determination of the strain gages resistance variation.

To perform a load cell calibration one should find the electric strain gages resistance variation law as a function of the mechanical loading or the external weight, pressure, deformation, etc. This law can be investigated by experimental meanings or derivates from data supplied by the manufacturer.

2. A BRIEF DISCUSSION ON DISPLACEMENT TRANSDUCER

Different devices can be incorporated to the systems of displacement measurement, for example, one can employ an electric generator (tachometer, dynamo or small DC motor) and use the induced voltage or current to have indirect determination of a given angular speed. By calculation, integrating along the time, it is possible to determine the total displacements.

A device that may be considered on the development of this kind of sensing system is the Linear Variable Differential Transformer (LVDT) as proposed by Shang-Teh Wu et al (2007), see "Fig. 1".

The LVDT uses the electromagnetic induction between two coils modified by a motion core. The variation of the induced current is converted in a voltage proportional to the core positioning and consequently on its displacement. Despite the fact that remains an expensive device, this sensor has high resolution and high linearity (Hareem Tariqa (2001)).

The physical principles of most of these sensors, as well as aspect related to detection and the interfacing circuits are described by Fraden, (2003). Looking through out that description it is clear that all cited transducers supply indirect information about the real displacement, that later will be changed on real positioning measurement using a specific algorithm and electric signals processing on converting the selected observable into the adequate displacement units and scale.

A simple displacement sensitive system, with very low cost, is the personal computer mouse as discussed by J. Palacin et al (2005). The displacements from both sensors (x and y) are converted on the 2-D space positions of the computing system cursor.

The mouse, displaced by hand, rolls the rubber sphere on a plain surface, this PC man-machine interface is then able to communicates and store this handy displacement on the PC. This simple sensor, using very basic principles is enough to measure, to store and quantify trajectories, demanding very simple calibration to be able to perform that measurement on the metric unit system.

Exploring the optical displacement sensors, one will be confronted to different difficulties:

1) The reflexive surface must be clean, exempt of any dirt; otherwise this would affect its functioning, based on light reflection.

2) Optical systems are very sensitive to external vibrations, which can increase focusing difficulties of reflected light. To minimize optical and mechanical issues, one can use optical encoders, on that kind of measuring device the encoding system could be made mechanically, using a slotted wheel, needing no mechanical contact between the measured plain surface, trajectory, etc and the sensor.

3) To guarantee a good encoder resolution it is necessary to have as many slots as possible on the encoding wheel or amplify its rotation by mechanical meanings, what requires mobile parts and mechanisms, creating additional technological difficulties.

A displacement linear sensor using strain gages as "Fig. 2" is proposed by Pradeep Kumar Dhiman at al (2006). It works depending on a deformable system, constituted by a restricted beam attached to its extremities, with an inserted pipe connected to a metallic rod. The system deformation causes the unbalancing of a Wheatstone bridge of strain gages, see Vyroubal, D, (1993). The device is calibrated as a function of the connecting rod deformation, so the system becomes able to measure the displacement in one direction. The main limitation of this system is the small course of the observable movement, around 10 mm.

Investigating the state of the art on linear displacement sensors shows you that the best displacement sensors are produced by Spage Age Control as "Fig 3". These transducers convert mechanical movements into electric signal using a potentiometer (pot), see figure 3, this transducer is usually called string-pot. The pot angular measurement is then transformed into linear displacement. This sensor has some repeatability limitations, especially when high speed is required.
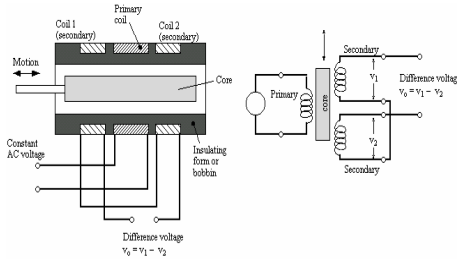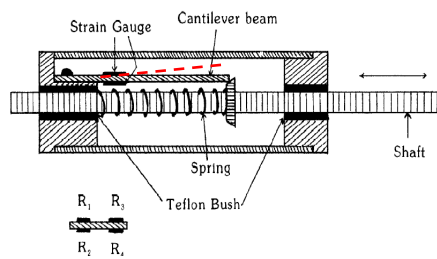

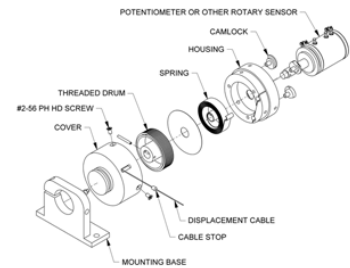| Figure 1. LVDT | Figure 2. Pradeep Kumar sensor | Figure 3. String pot sensor |

2.1. Displacement transducer choice

On developing a displacement sensor one should keep on mind several project requests as low cost, robustness, high repeatability, and good fold-back when submitted to repetitive load requests, high sensitivity, requesting of small volume for installation, good precision, and easy construction; the sensor may be assembled with the lesser number of mechanical parts; easy maintenance as "Tab. 1".

In this project phase the product is defined functionally and by specific principles methodologies, such as the Pugh concept analysis. Starting by identifying the diverse product creation solutions, one should be advised by a group of specialist jugging the best way to arrive on the final product. This judgment usually combines different techniques and alternatives conceptions.

Table 1. Relevant points on choosing a sensor

Guide to decision			
Parameter	**Choices**		
Contact	Contact	Noncontact	
Motion Type	Linear	Rotary	
Dimensions	One Dimensional	Multidimensional	
Measurement Type	Absolute	Incremental	Threshold (Proximity)
Range	< 1"	1" - 30"	> 30"
Size/Weight	Size Restriction____	Weight Restriction____	
Environment	Humidity	Vibration	Corrosion	Temperature
Installation/Mounting	Removable	Installation	Time Limit_____
Accuracy	Linearity	Resolution	Repeatability	Hysteresis
Lifetime	Cycles_____	Hours of Continuous Operation___	
Cost	< $50	$50 - $500	> $500
Output	Voltage	Current	Digital	Visual
Freq. Response	< 5 Hz	5 - 50 Hz	> 50 Hz

2.2. Choice of the displacement sensor

The intention of this work is define, project, develop and mount a displacement sensor that has a good precision and low cost associated.

The Pugh decision matrix was used to identify the optimum conceptual system. Initially were designed five sensors as "Fig. 4" for an evaluation based on the decision guide tool as "Tab. 2".
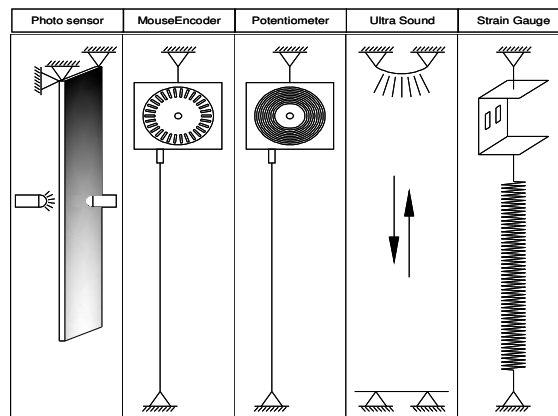

Figure 4. Studied sensors

The first proposition is a photo sensor. The device emits and receives light through a blade filled with gradient shading in two colors. The blade movement is enough to change the photocurrent on the optical receiver, as a function of the blade optical density.

The second proposition is a personal computer Mouse converted on optical encoder, to do so, a PC regular mouse was used and on that case, both electronic and mechanical parts are employed. An external nylon wire, associated to the PC mouse mechanism, produce a rotation encoder. A calibration routine is necessary to define the relation between the number of rotations and the linear displacement.

The tryout number three was a position encoder based on a potentiometer. This transducer is assembled using mechanical parts of the PC mouse as well. The difference between propositions numbers two and three is the replacement of the optical ensemble by a potentiometer.

As prototype number four, an ultra sound cell has been developed and mounted as displacement measuring system. This sensor produces an ultra sound around 50K Hertz that is reflected on a plane surface.

Finally a load cell based on strain gages is developed and assembled, that is proposition number five. To increases the total displacement range of the final transducer a steel spring has been associated to the load cell. Once one is using the intrinsic mechanical properties of the spring, it is necessary to know the spring elastic constant before make the load cell calibration. That calibration will establish the relation between the developed load cell response to an external exciting force and the mechanical displacement.

Table 2. Pugh concept analysis to select a displacement transducer

Criteria		1 Photosensor	2 Encoder / Mouse	3 Potenciometer	4 Ultra Sound	5 Strain Gauge
Cost		1	1	-1	1	-1
Accuracy		1	1	1	-1	1
Answer to excitation		1	1	1	1	1
Durty accumulation		1	1	1	-1	1
Construction		-1	1	1	-1	-1
Instalation easiness		-1	-1	-1	-1	1
Amount of mechanical parts		-1	-1	-1	0	1
Maintenance		-1	-1	-1	1	0
Repeatability		1	1	1	1	1
Value = +1 = High / Good	Σ+	+5	+6	+5	+4	+6
Value = 0 = Indifferent	Σ—	-4	-3	-4	-4	-2
Value = -1 = Low / Bad	Σ	1	3	1	0	4

Table 2 shows that the best choice on displacement transducer is the one based on strain gage, therefore presents the best score on the 6 sigma decision matrix. This technical solution will be adopted and developed along this paper.

3. LOAD CELL TRANSDUCER DESIGN

The numerical modeling results, obtained by finite element method, were used to design the aluminum profile used as the load cell body. These values are compared to the analytical calculation, see Avril, 1974.

The parts pre-dimensioning were done to define the proposed load cell capacity first. Its dimensioning is made using the theoretical formulations for plates supplied by Timoshenko & Woinowsky (1959).

Initially it was verified the validation of the theoretical results comparing the elastic deformation on the strain gages, with the maximum deflection and stress at a given portion or load cell region. The software template Abaqus was used to perform the linear static analysis.

The numerical model used is based on a shell of elements and some boundary conditions as: material (aluminum), thickness (1.84 mm) and the exciting loads on nodes A and B (10 N) as "Fig. 5".
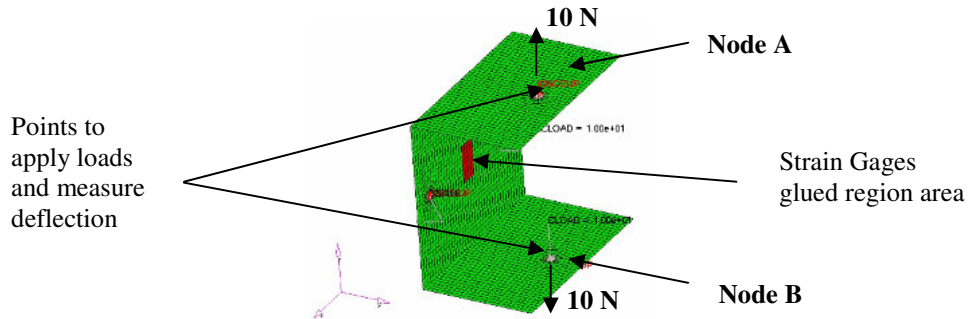

Figure 5. Finite Element Model (FEM)

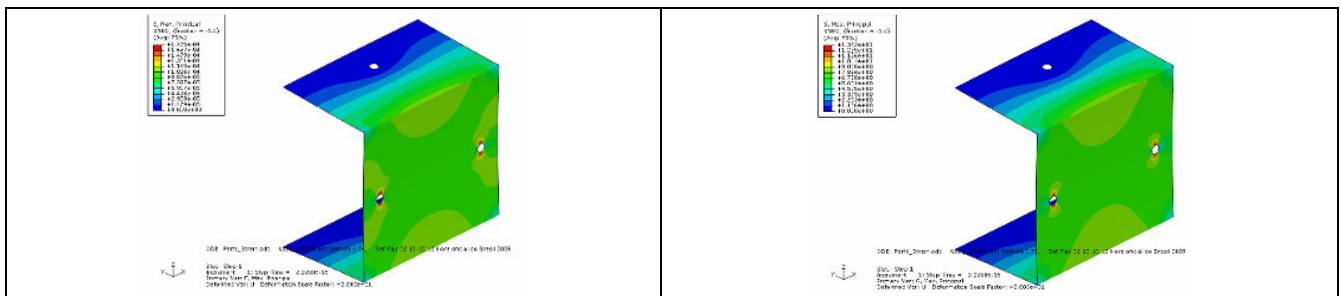The FEM results are showed on the "Figures 6, 7, 8 and 9".

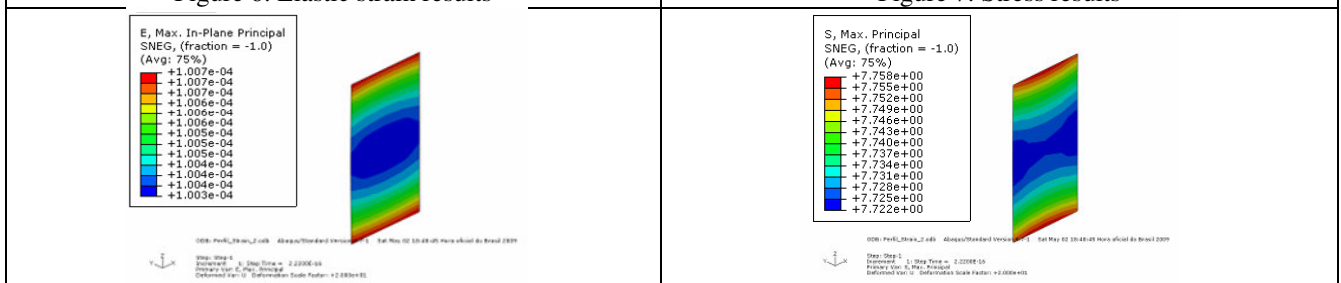| Figure 6. Elastic strain results	Figure 7. Stress results
Figure 8. Elastic strain on the strain gages region	Figure 9. Stress on the strain gages region

The twice times 10 N loads were used to, keeping the system stable, perform a linear static analysis. In principle, any load value could be used, but it is important to observe the linearity of the modeling. This information is very useful to guarantee that elastic limits are not exceeded, generating undesirable plastic deformation on the load cell mechanical structure and on the strain gages.

When deformation limits are exceeded more than material yield stress, plastic deformation appears and the strain gages are not anymore able on making a good strain measurement. The aluminum yield stress is around 100 MPa. "Fig. 10" shows the geometrical dimensions of the deformable element.

Based on that figure, one can write the analytical expression:

$$\varepsilon i = \frac{F}{E \times a \times e} \times \left(\frac{6 \times c - 1}{e} \right) \quad (1)$$

$$\Delta b = \frac{4 \times F \times c^2}{E \times a} \times \left(\frac{3 \times b}{e^3} + \frac{2 \times c}{d^3} \right) \quad (2)$$
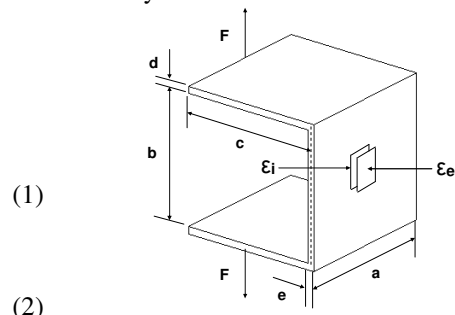
Where:

Figure 10. Geometrical profile dimensions

ε_i - internal strain; ε_e - external strain - $\varepsilon_e = -\varepsilon_i$

E - elastic modulus = 70,000 MPa

a – width profile = 40.00 mm

b – height = 34.66 mm

c – length = 17.08 mm (distance of load application)

d = **e** = thickness = 1.84 mm

e – thickness = 1.84 mm; Δb – deflection

Table 3. Stress and strain results

Element Label	Max.Principal Strain at integration point	Max. Principal Stress at integration point [MPa]
1091	1.0075E-04	7.7601
.	.	.
.	.	.
.	.	.
3492	1.0063E-04	7.7458
Average	**1.01E-04**	**7.7446**

Table 4. FEM deflection between nodes A and B

		Coordinates			Relative displacements		
	ID Node	X	Y	Z	X	Y	Z
Before applied loads	3389	20.000	-7.001	2.000			
	3728	20.000	-7.001	-38.236			
					0.0000	0.0000	**0.0925**
After applied loads	3389	20.000	-7.001	2.046			
	3728	20.000	-7.001	-38.282			

"Tab. 3" shows the results for the strain gages (SG) glued region area. Highlighted results, for the deformation and stress on the strain gages region, could be compared with the analytical calculations. On "Tab. 4" one can see on the relative displacement results between nodes A and B. "Tab. 5" shows the comparisons between FEM results and analytical calculation. Finally, "Tab. 6" shows the analytical calculation using FEM inputs, compared with maximum principal strain from "Tab. 3".

Table 5. Comparisons between FEM and analytical calculations

Parameter	FEM results	Analytical calc.	Diff
Δb **[mm]**	0.0925	0.0924	**0.14%**
ε [strain]	1.0060E-04	1.0705E-04	**-6.41%**

Table 6. Analytical calculations with FEM results

E [MPa]	a [mm]	b [mm]	c [mm]	d [mm]	e [mm]	F [N]	Delta b [mm]	Ee=-Ei [strain]	Stress [MPa]
70000	40.00	34.66	17.08	1.84	1.84	2.00	0.0185	2.14E-05	1.549
70000	40.00	34.66	17.08	1.84	1.84	4.00	0.0370	4.28E-05	3.098
70000	40.00	34.66	17.08	1.84	1.84	6.00	0.0554	6.42E-05	4.647
70000	40.00	34.66	17.08	1.84	1.84	8.00	0.0739	8.56E-05	6.196
70000	40.00	34.66	17.08	1.84	1.84	10.00	0.0924	1.07E-04	7.745
70000	40.00	34.66	17.08	1.84	1.84	12.00	0.1109	1.28E-04	9.293
70000	40.00	34.66	17.08	1.84	1.84	14.00	0.1294	1.50E-04	10.842
70000	40.00	34.66	17.08	1.84	1.84	16.00	0.1479	1.71E-04	12.391

4. THE LOAD CELL CONSTRUCTION

A commercial aluminum profile has been used as the load cell (LC) body on this experiment, to define its dimensions one have performed a previous analytical calculations (see item 4). The critical dimensions, those that can be varied and adjusted as free parameter, were "a" the width and "c" or the distance from the cell center and the load application point. The previous experiments showed that the most sensitive dimension was the load application point (c). It implies on the most severe load cell body (aluminum profile) deformation. See "Figures 11 and 12".
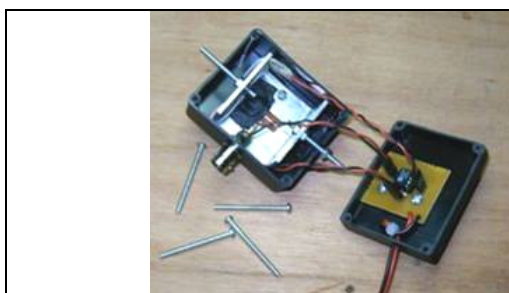

Figure 11. Load cell prototype and amplifier circuit	Figure 12. Load cell and amplifier circuit in a box

Inside the LC body, four 6mm, 120Ω strain gages, were positioned and glued. The strain gages gluing location can maximize the electric sensitivity, minimalizing measurements errors and decreasing the LC temperature dependence. A Wheatstone bridge consists of the 4 electrical resistances connected together (in this in case the 120Ω strain gages), as shown on figure 13.

Applying Ohm's law, on can write the following expressions:

$$Eo = \left[\frac{R1 \times R4 - R2 \times R3}{(R1 + R2) \times (R3 + R4)} \right] \times E \qquad (3)$$

$$\frac{R1}{R2} = \frac{R3}{R4} \qquad (4)$$

The null condition is satisfied when the Wheatstone bridge is balanced as "Eq. (4)". For the unbalanced Wheatstone bridge, on "Eq. (3)", one can see that the output voltage is 4 times bigger than the voltage produced by one active strain gage. It means that the proposed displacement sensor will be 4 times more sensitive for a given deformation.

"Fig. 14" shows the mechanical aspect of the strain gage transducer employed on the load cell construction. Uniaxial SG type has been used to measure strain in one direction.

a – carrier material
b – measuring grid
c – connections
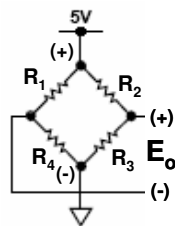d – effective grid lenght
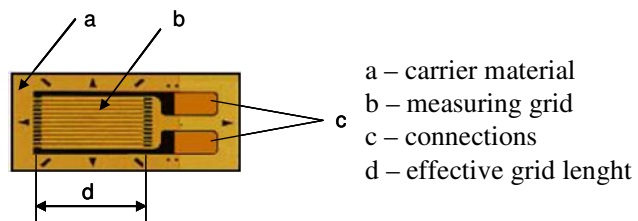
Figure 13. Wheatstone bridge   Figure 14. Strain gage model

For the strain gages gluing the choice of adhesives must be done before starting the load cell construction, one can use isocyanate super-glue or a two components epoxy. Once decided the glue, the aluminum body surface must be cleaned and then the strain gage gluing location should receive a clear reference mark to avoid mistakes. Glue strain gages on the clean surface, make some pressure for a while and live the adhesive curing. After, one can star the wires connections and the SG electrical isolation verification. Finally the glued transducer could be covered with RTV (silicone) to avoid humidity.

5. LOAD CELL TESTS AND CALIBRATIONS

The strain gage output signal is generally small, less then some microvolt. It is necessary to amplify and filter this signal before applying it to a data acquisition system. "Fig. 15" shows the usual process sequence permitting that a signal from a physical phenomenon, treated and interpreted adequately, becomes a trustable measurement.
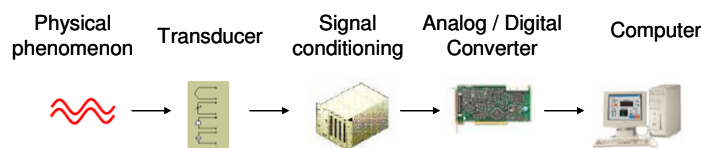

Figure 15. The measurement system

Most of the physical observables are measured indirectly by analogy or comparison between a given parameter and the given physical quantity, to do so, one needs a calibration routine permitting the analogy.

Two systems has been developed to calibrate the displacement transducer, the first one was an analog to digital converter (ADC, the ADS7804 produced by Texas Instrument) droved by a homemade software. The second system was a mechanical device capable to generate and repeat controlled displacements.

5.1. Calibrating and testing the developed device

The calibration setup is shown on "Fig. 16". On that figure one can see the prototype (load cell), the signal processing and data acquisitioning system (pre-amplifier, low pass filter, ADC and a personal computer) and the mechanical test template. To power up the system two DC power supplies has been used.

Figure 16. The repeatability test device

The pre-amplifier: for pre-amplifying the signal from the load cell one has used the Analog Device, AD 623 – Single supply instrumentation amplifier. Its simplified schematic is shown on "Fig. 17". The pre-amplify gain, set by R_G, is 100. The pre-amp electronic circuit, as well as the load cell circuitry, is represented on "Fig. 18".
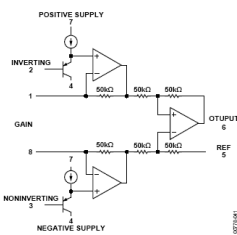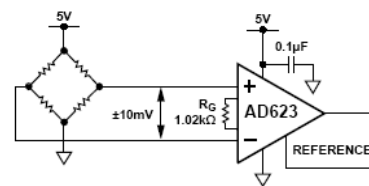

Figure 17. AD 623 (Analog Devices)

Figure 18. Electronic scheme (Analog Devices)

Low pass filter: The low pass filter used to cut high order harmonics and high frequency noise is a sample RC, first order, circuit with a cut-off frequency of 10 Hz.

ADC characteristics: The analog to digital converter has two analog inputs, readout by the PC parallel port, 12 bits resolution (counting from -2047 to +2047), full scale input voltage = 1 V, what implies a 0.24414 mV sensitivity, symmetrically powered by +12 V to -12 V; high electrical noise rejection, with four additional selectable gains for each channel.

The mechanical device for repeatability tests: The power used for moving this mechanical device comes from a 12VDC motor connected to a graduated eccentric arm, see "Fig. 19", the elastic coupling between the motor and the arm is done by roller bearings. Rigid brackets are used to support the induced displacement efforts on the transducer. The whole structure is mounted on four adjustable and anti vibration feet.
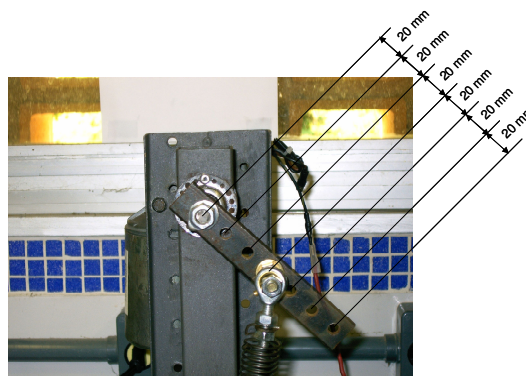

Figure 19. Graduated eccentric arm

The electric motor produces the rotation of the eccentric arm creating a quasi-sine mechanical movement, this periodic displacement pass by distinct maximum and minimum points. These two maxima are used to calibrate the connection spring displacement. This spring transfer movement to the prototype arm, the displacement amplitude can be changed using the equidistant holes on the graduated arm. During the tests 4 holes were used: Positions 01, 02, 03 and 04. The load cell output signals were acquired for a frequency of 100 Hz, within 20s for each data taking run. "Fig. 20" shows to the results; the displacement amplitude measured with the developed sensor is scaled on ADC counts units. For each position were realized 30 measurements and peaks has been recorded (maximum and minimum).

5.2. Sine waves generator:

In order to perform the ADC electrical calibration, a low frequency sine-wave generator has been employed. "Fig. 21" shows the results for sine waves data acquisition. On this procedure a digital oscilloscope was used to calibrate the ADC in terms of real voltage, one has used the same dynamic interval as the excitation produced by the mechanical test device (around 10 Hz).
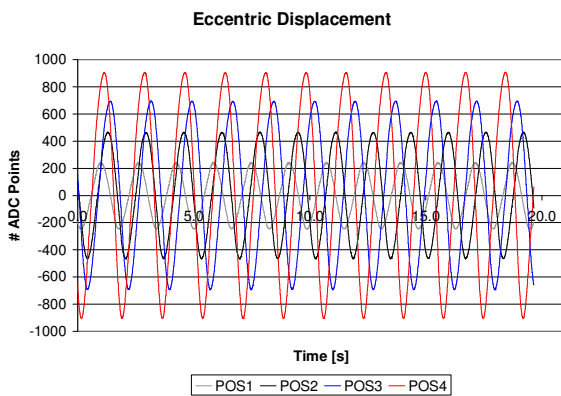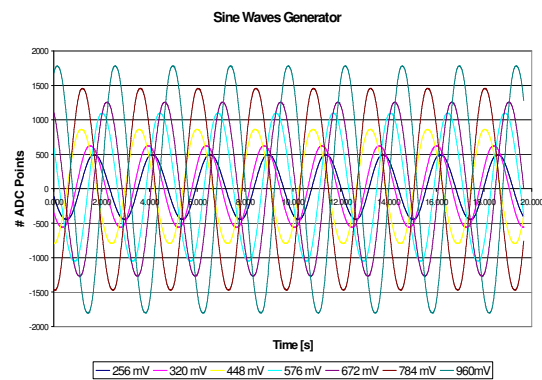

Figure 20. Eccentric displacement results

Figure 21. Vpp results

"Tab. 7" and "Fig. 22" show the displacement calibration results. The final calibration equation for the sensor, relating ADC counts and real mechanical displacement is describe on "Eq. (5)":

$$D [mm] = 0.08725781 * ADC\ counts \tag{5}$$

Table 7. Displ. results   Table 8. Sine wave Peak to Peak voltage X ADC counts

# ADC Points	Max/Min Peaks
-905	-80
-692	-60
-466	-40
-246	-20
246	20
466	40
692	60
905	80

Vpp [mV]	# ADC Points
-480	-1791
-392	-1462
-336	-1261
-288	-1072
-224	-828
-160	-590
-128	-469
128	469
160	590
224	828
288	1072
336	1261
392	1462
480	1791
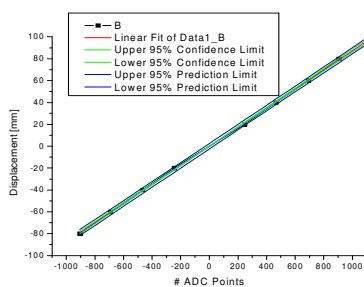
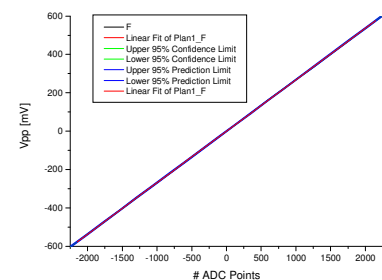Figure 22. Displacement calibration results   Figure 23. Vpp calibration results

"Tab. 8" and "Fig. 23" show the sine wave generator calibration results.
"Eq. (6)" shows the relation between the numbers of ADC counts and real peak to peak voltage (mV) acquiring the sine wave signals.

$$Vpp [mV] = 0.26826942 * ADC\ counts \tag{6}$$

5.3. Repeatability verification

Un important parameter on determining a sensor final quality is the repeatability, in principle the sensor behave would not change from one measuring cycle to another, even if the sensor exhibit some hysteresis component. "Tables 9, 10 and 11 show the statistical results obtained from measurements using the mechanical template (test machine). The

one-way analysis of variance (ANOVA) and the Scheffe tests were used to compare the difference between data acquired during different experimental runs, also call "group".

Table 9. Statistical values

SUMMARY				
Groups	Count	Sum	Average	Variance
group 1	30	7005	233.50	0.948276
group 2	30	6995	233.17	0.057471
group 3	30	7002.333	233.41	0.074202
group 4	30	7000.75	233.36	0.033118

Table 10. ANOVA

ANOVA						
Source of Variation	SS	df	MS	F	P-value	F crit
Between Groups	1.787674	3	0.595891	2.141	0.0988	2.683
Within Groups	32.27894	116	0.278267			
Total	34.06661	119				

Table 11. Scheffe Test Tesults

Summary of Scheffe Test Results			
	F		F crit
Group 1 versus Group 2	1.996	<	2.683
Group 1 versus Group 3	0.142	<	2.683
Group 1 versus Group 4	0.361	<	2.683
Group 2 versus Group 3	1.074	<	2.683
Group 2 versus Group 4	0.660	<	2.683
Group 3 versus Group 4	0.050	<	2.683

Group1 to 4 refer to Position 1 to 4 on the graduated eccentric arm ("Fig. 19"). Basically the statistical tests investigate differences between the means value of several populations.

Using statistical knowledge on can formulate a null and the alternative hypothesis described below:

H_0: $\mu1 = \mu2 = \mu3 = \mu4$

H_A: $\mu1 \neq \mu2 \neq \mu3 \neq \mu4$ (the means values are not all equal)

Based on Scheffe test the null hypothesis H_0 will be rejected if F is $>= F_{crit}$. In this case any combinations of all groups values are minor than F_{crit} and then does not exist a significant difference between meaning values, so, the null hypothesis could be accept, and the t-test could be used as well.

The statistical analysis was done in order to verify the repeatability results acquired using the developed sensor, where strain gages; assembled on the load cell; are used with displacement measuring propose. Minitab statistical software and excel spreadsheet were used as numerical template for this analysis.

Based on the results obtained (see "Tab. 11"), it could be established that a very good repeatability was obtained and this parameter can be associate to the linear behave of the strain gage ensemble.

5.4. Relation between displacement and output voltage

Considering the two "Eq. (5) and (6)", it can be observed an excellent linearity and repeatability on the load cell (LC) behave and measurement results. Dividing "Eq. (6)" by "Eq. (5)", one will find the relation between displacement and the LC and the readout system output voltage.

*Vpp [mV] = 3.074445944 * D [mm]*   (7)

This equation, determined throughout the calibration routine, is indispensable on characterizing the developed sensor and will be very useful on different applications, like displacement control, unbalanced load charging on mechanical structures and structure overload alarms.

6. FINAL COMMENTS AND CONCLUSIONS

It is important to point out that the level of accuracy achieved, on the displacement measurements, using the developed sensor is close to the commercial standards as string pot. In the present work it was developed and calibrated a data acquisition system based on the ADS 7804AP (TEXAS Instrument), as well as its software driver. The developed system has been characterized at 100 Hz and gives good results.

One important aspect was the development of technical skills and technology on gluing strain gage to metal surfaces.

During the prototyping phase, the spring stiffness value was obtained from experimental data and resulted k = 0.20902. Using the equation F [N] = 0.20902 * x, where "x" is spring displacement, for a stroke of 160 mm, the spring force was equal to 33.44 N. This value can be compared with the analytical results presented on table 7. By analytical calculation one will find 32 N and the stress value is 12.39 MPa, this calculation is based on the linear stress analysis. The total displacement measurement achieved by the developed sensor was 160 mm, due to some mechanical

restrictions; the authors would point out that a similar system could measures up to 250 mm. This affirmation is supported by the excellent linearity achieved by the prototype.

Considering a displacement equal to 250 mm, the effort on the prototype will be 52.26 N and stress value equal to 20.24 MPa. This value is very small compared to 100 MPa of the yield stress characteristic of the aluminum profile used on the prototype load cell body.

Another important factor observed was the low budget spent on this work, compared to the budget for buying a commercial displacement sensor. The sales price for a similar devices supplied by national and international manufacturers is at least 50 times more expensive.

In conclusion, a displacement transducer based on strain gage, with good accuracy and linearity, for measurements on the range from 0 to 250 mm has been designed, developed, fabricated, calibrated and tested. This general proposes sensor can be used on many different applications, specially where low budget and high accuracy are required.

7. ACKNOWLEDGEMENT

8. REFERENCES

ABAQUS Simulia Documentation Release 6.7-4

Avril, Jean Malakoff : Vishay-Micromesures, 1974. Encyclopédie Vishay d'analyse des contraintes

Blanchard B. S. & Fabrycky W. J. Systems Engineering and Analysis. Prentice – Hall, 1990. Kano, N., Attractive quality and must-be quality, The Journal of the Japanese Society for Quality Control, April, pp. 39-48, 1984.

Fraden, Jacob, 2003 "Handbook of modern sensors: physics, designs, and applications", Advanced Monitors Corporation 6255 Ferris Square, Suite M San Diego, CA 92121 USA

Hareem Tariqa,b, Akiteru Takamoria, 2001, "The linear variable differential transformer (LVDT) position sensor for gravitational wave interferometer low-frequency controls" , a LIGO project, California Institute of Technology, 1200 E. California Blvd, Pasadena, CA 91125, USA

J. Palacin, I. Valganon, R. Pernia, 2005, "The optical mouse for indoor mobile robot odometry measurement" ,Departament d'Inform`atica i Enginyeria Industrial, Universitat de Lleida, Jaume II, 69, 25001 Lleida, Spain Received 27 April

Pradeep Kumar Dhiman1, Kirat Pal2 and R. K. Sharma1, "Gage Based Displacement Sensor", 1Department of Physics, D.A.V. (P.G.) College, Dehradun-248001, 2Earthquake Engineering Department, I.I.T. Roorkee, Roorkee-247667, India, email : kiratfeq@iitr.ernet.inStrain

Pugh, S - Total Design: Integrated Methods for Successful Product Engineering, Addison Wesley, 1991.

Shang-Teh Wu, Szu-Chieh Mo, Bo-Siou Wu, 2007, "An LVDT-based self-actuating displacement transducer" ,Department of Mechanical Engineering, National Yunlin University of Science & Technology, Touliu, Yunlin 640, Taiwan

SpaceAge Control, "String Potentiometer and String Encoder Engineering Guide", 2006, http://www.spaceagecontrol.com/Litroom

Holmberg, P., Automatic balancing of linear ac bridge circuit for capacitive sensor elements, IEEE Trans. Inst. & Meas. Vol. 44 No. 3, June 1995, pp. 803-805.

9. RESPONSIBILITY NOTICE

The authors are the only responsible for the printed material included in this paper.